

Substituting Leucine for Alanine-86 in the Tether Region of the Iron–Sulfur Protein of the Cytochrome *bc*₁ Complex Affects the Mobility of the [2Fe2S] Domain[†]

Mousumi Ghosh, Yudong Wang, C. Edward Ebert, Satya Vadlamuri, and Diana S. Beattie*

Department of Biochemistry, West Virginia University School of Medicine, Morgantown, West Virginia 26506-9142

Received July 24, 2000; Revised Manuscript Received October 9, 2000

ABSTRACT: Mutating three conserved alanine residues in the tether region of the iron–sulfur protein of the yeast cytochrome *bc*₁ complex resulted in 22–56% decreases in enzymatic activity [Obungu et al. (2000) *Biochim. Biophys. Acta* 1457, 36–44]. The activity of the cytochrome *bc*₁ complex isolated from A86L was decreased 60% compared to the wild-type without loss of heme or protein and without changes in the 2Fe2S cluster or proton-pumping ability. The activity of the *bc*₁ complex from mutant A92R was identical to the wild-type, while loss of both heme and activity was observed in the *bc*₁ complex isolated from mutant A90I. Computer simulations indicated that neither mutation A86L nor mutation A92R affects the α -helical backbone in the tether region; however, the side chain of the leucine substituted for Ala-86 interacts with the side chain of Leu-89. The Arrhenius plot for mutant A86L was apparently biphasic with a transition observed at 17–19 °C and an activation energy of 279.9 kJ/mol below 17 °C and 125.1 kJ/mol above 17 °C. The initial rate of cytochrome *c*₁ reduction was lowered 33% in mutant A86L; however, the initial rate of cytochrome *b* reduction was unaffected, suggesting that movement of the tether region of the iron–sulfur protein is necessary for maximum rates of enzymatic activity. Substituting a leucine for Ala-86 impedes the unwinding of the α -helix and hence movement of the tether.

The cytochrome *bc*₁ complex,¹ an integral multiprotein complex of the inner mitochondrial membrane, catalyzes the transfer of electrons from ubiquinol to cytochrome *c* coupled to the translocation of protons across the membrane (1–3). The *bc*₁ complex of yeast mitochondria consists of 10 subunits, of which 3 have prosthetic groups that serve as redox centers, cytochromes *b* and *c*₁ and the Rieske iron–sulfur protein. The transfer of electrons through the *bc*₁ complex is best explained by the Q-cycle mechanism (5–7) in which four protons are translocated across the mitochondrial membrane per two electrons transferred from ubiquinol to cytochrome *c*. For electron transfer to continue according to the Q-cycle, two separate ubiquinone or ubiquinol binding sites are required in the *bc*₁ complex. A ubiquinol oxidizing site (Q_O) is located at the positive (P) side of the membrane and a ubiquinone reducing site (Q_I) at the negative (N) side of the membrane. The oxidation of ubiquinol at the Q_O site

results in the transfer of one electron to the 2Fe2S cluster of the iron–sulfur protein, which subsequently is oxidized by transfer of an electron to the heme of cytochrome *c*₁. The strongly reducing ubisemiquinone anion formed during ubiquinol oxidation in the Q_O site immediately reduces the low-potential heme of cytochrome *b*_L that rapidly transfers an electron to the high-potential heme of cytochrome *b*_H. The reduced cytochrome *b*_H is then oxidized by transfer of an electron to either ubiquinone or ubisemiquinone at the Q_I site.

The recent resolution of the crystal structure of the cytochrome *bc*₁ complex from beef (8, 9), chicken (10), and yeast mitochondria (11) has revealed that the *bc*₁ complex exists as a dimer with the eight membrane-spanning helices of cytochrome *b* comprising the core of the complex. In the crystal structure, the iron–sulfur protein consists of three separate domains: a membrane-spanning α -helix at its N-terminus passing through the membrane at an angle, a soluble extramembranous domain containing the bulk of the iron–sulfur protein including the 2Fe2S cluster, and a “tether” of eight amino acids connecting the extrinsic domain to the membrane-spanning α -helix (9, 10).

The subsequent resolution of three different conformations of the iron–sulfur protein in the *bc*₁ complex indicated that this protein can exist in different positions in the complex depending both on the crystal form on and the presence of

[†] This work was supported, in part, by National Institutes of Health Grant GM 57213.

* To whom correspondence should be addressed at the Department of Biochemistry, P.O. Box 9142, West Virginia University School of Medicine, Morgantown, WV 26506-9142. Tel: 304-293-7522, FAX: 304-293-6846, E-mail: dbeattie@hsc.wvu.edu.

¹ Abbreviations: cytochrome *bc*₁ complex, ubiquinol:cytochrome *c* oxidoreductase; CCCP, carbonyl cyanide *m*-chlorophenylhydrazone; DBH₂, 2,3-dimethoxy-5-methyl-6-decyl-1,4-benzoquinol; DM, dodecyl maltoside; SDS–PAGE, sodium dodecyl sulfate–polyacrylamide gel electrophoresis; SMP, submitochondrial particle.

86	90	92	
T	A	D	<i>S. cerevisiae</i>
S	A	D	
S	A	D	<i>N. crassa</i>
S	A	D	
T	A	D	<i>B. taurus</i>
T	A	D	
S	A	D	<i>H. sapiens</i>
S	A	D	
S	A	D	<i>R. capsulatus</i>

FIGURE 1: Sequence alignment of amino acids in the tether region of the iron–protein of the cytochrome *bc*₁ complex from different species (16). The vertical lines indicate the conserved alanine residues (Ala-86, Ala-90, and Ala-92) that were mutated.

Q_O site inhibitors. These observations have suggested the possibility that the extrinsic domain of the iron–sulfur protein might undergo movement during electron transfer (4, 9–12). A model that explains electron transfer through the *bc*₁ complex in light of the crystal structure suggests that when ubiquinol binds in the Q_O site and is deprotonated, the headgroup of the iron–sulfur protein moves closer to cytochrome *b* and assumes the ‘*b*’ state. The ‘*b*’ state involves ligand formation between His-161 of the 2Fe2S binding cluster on the iron–sulfur protein and the carbonyl and methoxy oxygens of the ring system of stigmatellin (13), an inhibitor that is bound to cytochrome *b* at the distal ubiquinol binding pocket (14). The deprotonated ubiquinol bound at the Q_O site then undergoes oxidation through a concerted mechanism in which one electron is transferred to the iron–sulfur protein and the second electron immediately transferred to heme *b*_L and subsequently to heme *b*_H (15). The ubiquinone thus formed is released from the Q_O binding pocket followed by the subsequent movement of the reduced iron–sulfur protein to the ‘*c*₁’ state close to the heme of cytochrome *c*₁ where rapid electron transfer from the 2Fe2S cluster to heme *c*₁ occurs (12, 13).

Despite the changes in the position of the 2Fe2S cluster of the iron–sulfur protein, the crystal structure has indicated that the conformation of the membrane-spanning helix remains unaffected under all experimental conditions. The conformation of the headgroup of the protein also remains unchanged in both the ‘cytochrome *b*’ (11) and ‘cytochrome *c*₁’ (9) positions, but shows a minor 2 Å shift in the intermediate position (9). This observation suggests that movement of the 2Fe2S cluster during electron transfer results mainly from the rotation of the entire head domain of the iron–sulfur protein. The flexibility to allow this rotation must come from the eight amino acids present in the “tether” region connecting the head domain to the transmembrane. The tether domain, a highly conserved region of the iron–sulfur protein, has the sequence TADVLAMA in yeast, amino acids 85–92 in the yeast numbering system (16). The presence of several highly conserved amino acid residues, including three alanines, in this region of the protein suggests that these small amino acid residues may provide the needed flexibility for the proposed stretching of the tether (Figure 1). In support of the need for flexibility in the tether region, a recent report has indicated that substituting two prolines for two alanines, 90 and 92, or three prolines for residues 86–88 resulted in an almost complete absence of electron transfer through the *bc*₁ complex of *Rhodobacter sphaeroides* (17). Further evidence for the movement of the flexible tether involves double cysteine mutants of *R.*

sphaeroides in which the loss of enzymatic activity was shown to result from disulfide bond formation, which would increase the rigidity of the tether region (18). Other approaches to understanding the role of the flexible tether in electron transfer have included using site-directed mutagenesis to either shorten or lengthen the tether as well as to change individual conserved amino acid residues in the tether. These changes resulted in variable decreases in enzymatic activity of the *bc*₁ complex (19–21).

In a recent study in our laboratory (20), we investigated the role of the conserved amino acid residues Ala-86, Ala-90, and Ala-92 located in the tether region of the yeast iron–sulfur protein (83-ATADVLAMA-92) by constructing site-directed mutations of these residues (Figure 1). The results indicated that the enzymatic activity of the *bc*₁ complex was reduced between 22 and 56% in all these mutants, although no loss of cytochromes *b* or *c*₁ was detected spectrally. In addition, quantitative immunoblotting revealed no significant loss of the iron–sulfur protein in any of these mutants with the exception of mutants of Ala-92. In all substitutions of Ala-92, the loss of enzymatic activity of the *bc*₁ complex paralleled the loss in the amount of the iron–sulfur protein. In the current study, the cytochrome *bc*₁ complex has been isolated and characterized from three of these alanine mutants (A86L, A90I, and A92R) that had reduced electron transfer activity through the *bc*₁ complex. The results obtained suggest that the loss of activity in the A86L mutant may occur because of steric hindrance that occurs between the substituted leucine at residue 86 and the conserved leucine present at position 89. By contrast, the *bc*₁ complex isolated from mutant A92R is essentially identical to the complex isolated from wild-type cells.

MATERIALS AND METHODS

Materials. Decylubiquinone (DB),¹ carbonyl cyanide *m*-chlorophenylhydrazone (CCCP), antimycin, valinomycin, and stigmatellin were purchased from Sigma Chemical Co. Dodecyl maltoside (DM) was purchased from Anatrace Inc. All other chemicals were of the highest quality available.

Growth of Yeast Cells and Preparation of Mitochondria. Yeast cells were grown to mid-logarithmic phase in a medium containing 1% yeast extract, 2% peptone, and 2% galactose ($A_{650\text{ nm}} = 1.0\text{--}1.4$) in 4 L flasks. Twenty liters of the cell culture was harvested by centrifugation at 4200g for 5 min at 4 °C. The pellets were resuspended in 400 mL of disruption buffer consisting of 10 mM potassium phosphate, pH 6.6, 0.65 M sorbitol, 2 mM EDTA, and 0.2 mg/mL benzamidinium hydrochloride, a serine protease inhibitor, and were broken using the modified glass bead method (20) prior to isolation of mitochondria as previously described (22). The mitochondrial pellet was resuspended in a buffer containing 0.9% KCl, 50 mM potassium phosphate, pH 7.5, 1 mM EDTA, and 0.2 mg/mL benzamidinium hydrochloride and recentrifuged at 18000g.

Purification of Cytochrome *bc*₁ Complex. The final mitochondrial pellet was suspended in ice-cold 50 mM Tris·HCl buffer, pH 8.0, containing 1 mM MgSO₄, 10% glycerol, and 0.2 mg/mL benzamidinium hydrochloride (Buffer A) prior to sonication using a macroprobe and an output control set at position 8 (Heat Systems-Ultrasonics, Inc.). Two pulses of 45 s were used separated by an interval of 2 min to obtain

submitochondrial particles (SMPs). The sonicated mitochondria were centrifuged at 100000g for 45 min. The pellet containing the SMPs was resuspended in Buffer A containing 100 mM NaCl, DM, 0.7 mg/mg of mitochondrial protein, was added and the solution slowly stirred for 1 h at 4 °C. The solubilized mitochondria were loaded onto a 250 mL DEAE-Biogel A (Bio-Rad) chromatography column equilibrated with 50 mM Tris·HCl buffer, pH 8.0, containing 0.5% DM and 100 mM NaCl at a flow rate of 2.0 mL/min using an FPLC (fast performance liquid chromatography, Amersham Pharmacia Biotech). After loading, the column was washed with 2 volumes of the same buffer and eluted with 5 volumes of a linear gradient of 100–500 mM NaCl in 50 mM Tris·HCl, pH 8.0, at a flow rate of 1 mL/min. The cytochrome *bc*₁ complex was eluted with 350–450 mM NaCl. The fractions with cytochrome *c* reductase activity were pooled and applied at a flow rate of 2 mL/min on a prepacked 5 mL Hi-Trap Q column (Amersham Pharmacia Biotech) equilibrated with the same buffer as the first column. The column was washed with 4 volumes of 50 mM Tris·HCl, pH 8.0, containing 200 mM NaCl, followed by applying a gradient of 200–1000 mM NaCl (flow rate 5 mL/min) onto the column. The purified cytochrome *bc*₁ complex was eluted with 600–750 mM NaCl. The presence of subunits of the *bc*₁ complex was determined on a 15% SDS–PAGE stained with Coomassie Blue.

Enzyme Assays and Spectral Determination. The activity of the cytochrome *bc*₁ complex was determined by measuring the reduction of 40 μ M horse heart cytochrome *c* at 550 nm using the ubiquinol analogue decylbenzoquinol (DBH₂) as electron donor. The assay was performed at 25 °C in 50 mM Tris·HCl, pH 7.4, 1 mM EDTA, 250 mM sucrose, and 2 mM KCN. The enzyme reaction was initiated by the addition of 150 μ M DBH₂. The inhibition of enzyme activity by 1 μ M antimycin A and 1 μ M myxothiazol was determined for both the wild-type and the mutant enzymes. The rate of cytochrome *c* reduction was calculated using a molar extinction coefficient of 21.5 mM⁻¹ cm⁻¹ for cytochrome *c*.

The activation energy required for enzyme catalysis was determined for both the mitochondrial and purified enzyme preparations by determining the steady-state activity at temperatures between 10 and 35 °C at 2.5 °C intervals on a Cary 50 spectrophotometer equipped with a temperature controller. At each temperature, a minimum of three assays were performed and averaged. The activation energy was calculated from an Arrhenius plot.

Optical spectra for the purified *bc*₁ complexes were recorded using a Cary 50 Bio UV–Visible spectrophotometer. The cytochrome *c*₁ content was determined from the ascorbate-reduced minus ferricyanide-oxidized difference spectrum at 554–539 nm using an extinction coefficient of 24.1 mM⁻¹ cm⁻¹. The cytochrome *b* content was determined from the dithionite-reduced minus ferricyanide-oxidized difference spectrum at 563–575 nm using an extinction coefficient of 21.0 mM⁻¹ cm⁻¹.

Single-turnover measurements were performed at room temperature by rapid-scanning stopped-flow spectroscopy, using an OLIS modernized Cary 17 spectrophotometer equipped with an OLIS stopped flow. As the dead time of the instrument was 5 ms, this time was chosen as time 0, after which point data were collected. Reactions were started by mixing 1 mg/mL SMP in 50 mM potassium phosphate

buffer, pH 6.0, containing 250 mM sucrose, 0.2 mM EDTA, 1 mM NaN₃, and 1.0 mg/mL bovine serum albumin against an equal volume of buffer containing 150 μ M DBH₂. The time course of reduction of cytochromes *b* and *c*₁ was performed in the presence of 1 μ M antimycin at 563 and 554 nm, respectively. For each experiment, at least three data sets were averaged.

EPR Spectroscopy. EPR spectra of the 2Fe-2S cluster of the iron–sulfur protein in SMPs obtained from the A86L mutant and the wild-type were recorded using a Bruker EMX spectrometer equipped with a liquid N₂ Dewar at 77 K. The membranes were resuspended in 50 mM potassium phosphate, pH 7.5, 0.9% KCl buffer and reduced with 20 mM ascorbic acid under anaerobic conditions. Spectra were recorded both in the presence and in the absence of 25 μ M stigmatellin dissolved in dimethyl sulfoxide. EPR conditions were as follows: temperature, 77 K; microwave power, 0.05 mW; modulation amplitude, 6.0 G; modulation frequency, 100 kHz; and microwave frequency, 9.398 GHz.

Molecular Modeling. Molecular modeling was performed with an Octane Silicon Graphics station. The X-ray crystal structure for the cytochrome *bc*₁ complex isolated from *Gallus gallus* (PDB 1BCC) was downloaded from the Brookhaven Protein Data Bank (10). Unfortunately, the coordinates (1E2Y) for the crystal structure of the yeast *bc*₁ complex were not available at the time of this writing for use in this study (11). The region of the iron–sulfur protein corresponding to the flexible tether region sequence (SASA-DVLAMSK in bovine heart) was examined in detail. Amino acid substitutions to mimic appropriate mutations were made using the Biopolymer module from Insight II software (Molecular Simulations, Inc., San Diego). With the exception of the tether region, the entire molecule was fixed before energy minimization and molecular dynamics calculations were performed. The portion of the tether region that protruded into the aqueous extramembranous region was soaked with water using a sphere of 8 Å radius sufficient to soak the entire region of interest. Changes in the conformation of the tether region were examined using molecular dynamics as follows. Initially, energy minimization was performed on the tether region with the water added by soaking using a constant valence force field (cvff) and the method of steepest descents with a nonbond cutoff of 12 Å until the gradient was less than 1 kcal·mol⁻¹·Å⁻¹. Molecular dynamics simulations using the leapfrog algorithm were used; the system was equilibrated for 0.1 ps and the simulations continued for 5 ps at 300 K using 1 fs time steps with the same constraints. Structures were saved every 0.1 ps. Differences between mutant and wild-type conformations were examined by visual comparison (overlays) and distance measurements between reference atoms.

Preparation of Proteoliposomes Containing the *bc*₁ Complex and Measurement of Cytochrome *c* Reductase and Proton-Pumping Activity. Reconstitution of the purified *bc*₁ complex into phospholipid vesicles was performed by suspending 50 μ L of the purified complex containing 0.5 nmol of cytochrome *b* in 500 μ L of an ice-cold phospholipid solution containing 30 mM MOPS, pH 7.0, 0.5% sodium cholate, 30 mM *n*-octyl β -D-glucopyranoside, and 50 mg/mL soybean lecithin. The mixture was sonicated using a microprobe at an output control set at position 1 (Heat Systems-Ultrasonics, Inc.) for 10–15 s until the suspension

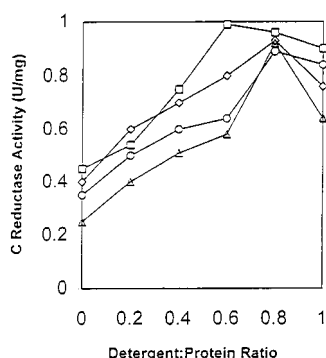


FIGURE 2: Effect of different concentrations of the detergent dodecyl maltoside (DM) on cytochrome *c* reductase activity of wild-type and mutants in the tether region of the iron–sulfur protein. Submitochondrial particles obtained from wild-type (□) and the mutants A86L (Δ), A90I (○), and A92R (◇) were treated with the indicated concentrations of detergent (mg of DM/mg of SMP) for 1 h at 4 °C. Enzyme activity was determined as cytochrome *c* reductase activity with DBH₂ as substrate.

appeared transparent. The sonicated mixture was incubated at 4 °C for 2–3 h prior to enzymatic assays.

Both cytochrome *c* reductase and proton-pumping activities were assayed at 25 °C in 2 mL of a medium containing 1 mM K-HEPES, pH 7.2, 100 mM KCl, 1 mM KCN, 7.5 μM cytochrome *c*, 1 μg of valinomycin, and 50 μL of the proteoliposomes. The reaction was started by addition of 150 μM DBH₂, prepared just prior to use by sodium borohydride reduction of DB. The rate of proton pumping was determined by the decrease in absorbance at 558 nm of the pH indicator dye Phenol Red (50 mM) resulting from the increase in proton concentration outside the proteoliposomes. Cytochrome *c* reductase activity in the proteoliposomes was assayed as the rate of cytochrome *c* reduction at 550 nm in the same medium minus the Phenol Red indicator. Liposomes prepared without any protein were used as controls for both assays.

RESULTS AND DISCUSSION

*Purification and Characterization of Cytochrome *bc*₁ Complex Isolated from Wild-Type and Mutant Yeast Strains.*

Prior to attempting the purification of the cytochrome *bc*₁ complex from mitochondria isolated from the iron–sulfur protein mutants, A86L, A90I, and A92R, which have decreased enzymatic activity (20), it was necessary to determine whether the *bc*₁ complex in these mutants was stable to detergent solubilization. Solubilization of the SMP membranes isolated from both wild-type and mutant yeast cells with increasing concentrations of DM resulted in 200–300% increases in the enzymatic activity of the solubilized *bc*₁ complex determined as cytochrome *c* reductase activity (Figure 2). The maximum enzymatic activity for the wild-type and all mutants was observed at a detergent-to-protein ratio of 0.6–0.8 mg/mg of SMP protein. The similar increases in enzymatic activity after detergent solubilization of mitochondrial membranes suggest that all three mutants are stable to DM extraction and hence should be amenable to further purification.

Purification of the cytochrome *bc*₁ complexes from the detergent-solubilized SMPs of the wild-type and mutant strains was accomplished by DEAE Biogel A and HiTrap Q column chromatography using an FPLC. A 10-fold

purification was observed for the complex from wild-type cells based on units per milligram of protein with a specific activity of 1.54 units/nmol of cytochrome *b* for the most purified fraction (Table 1). A comparable 10-fold purification of the *bc*₁ complex isolated from mutant A86L was observed with a specific activity of 0.62 unit/nmol of cytochrome *b* for the purified protein, a value that is decreased by 60% compared to the wild-type *bc*₁ complex. Purification of the *bc*₁ complex from mutant A92R resulted in a 13.0-fold purification such that the purified complex had a specific enzymatic activity essentially identical to that of the wild-type. By contrast, difficulties arose in our attempts to purify the *bc*₁ complex from mutant strain A90I as low yields and loss of enzymatic activity were observed such that the purified complex had a 73% decrease in specific activity compared to the complex from the wild-type yeast cells.

Characterization of the polypeptide composition of the purified *bc*₁ complexes from the wild-type and three mutant strains by SDS–PAGE revealed an identical subunit composition with no significant loss of any of the subunits including the iron–sulfur protein (Figure 3). Visible spectroscopy was used to determine the cytochrome *b* and *c*₁ heme contents of the *bc*₁ complexes isolated from the wild-type and mutant strains. The dithionite-reduced minus ferricyanide-oxidized difference spectrum indicated that the *bc*₁ complex isolated from wild-type and the three mutants strains had an α-band at 563 nm for cytochrome *b* and an α-band at 554 nm for cytochrome *c*₁ (Figure 4). The concentrations of cytochromes *b* and *c*₁ in the wild-type and the two mutants A86L and A92R were similar with a 1.6–1.8 ratio observed for the heme of cytochrome *b* relative to the heme of cytochrome *c*₁ (Table 1). This ratio is slightly lower than the theoretical value of 2.0 for the two hemes, suggesting that some loss of the *b* heme may have occurred during the purification process. By contrast, the *bc*₁ complex isolated from mutant A90I had lost significant amounts of both hemes *b* and *c*₁ during purification with a final heme *b*:*c*₁ ratio of 1.4. Due to the difficulties in purification, the low yields and loss of heme *b*, no further investigations of mutant A90I were performed.

To summarize the purification of the *bc*₁ complexes from the other two mutants, the *bc*₁ complex isolated from mutant A92R appeared to be identical to that isolated from the wild-type in terms of enzymatic activity, subunit composition, and heme content. These results support our previous conclusions that the loss of enzymatic activity observed in mitochondrial membranes of A92R correlated with the loss of the iron–sulfur protein. By contrast, the *bc*₁ complex isolated from mutant A86L had enzymatic activity decreased by 60% compared to the activity of the complex isolated from wild-type cells; however, this *bc*₁ complex appeared identical to the wild-type in terms of subunit composition and heme content. Further investigations of the *bc*₁ complex from mutant A86L were conducted in an attempt to establish the reason for the lowered activity in this mutant.

Effects of Stigmatellin on Mutant A86L. Examination of the crystal structure of the beef heart enzyme has indicated that Ala-86 is located at the start of the tether connecting the headgroup of the iron–sulfur protein with the membrane-spanning helix. In addition, Ala-86 is located near the end of the membrane-spanning helix adjacent to the *cd* helices of cytochrome *b*, which cover the quinol binding pocket

Table 1: Enzymatic Activities in Mitochondria and Purified Cytochrome *bc*₁ Complexes Isolated from Wild-Type and Mutants A86L, A901, and A92R of the Yeast Iron–Sulfur Protein^a

strain	growth rate ^b	specific activity						cytochrome content		
		mitochondria		purified complex				<i>b</i>	<i>c</i> ₁	<i>b/c</i> ₁ ratio
		units/mg of protein	% of control	units/mg of protein	% of control	units/nm of cyt <i>b</i>	% of control			
wild-type	2.0	0.65	100	6.7	100	1.54	100	4.35	2.80	1.6
A86L	3.0	0.31	48	2.6	39	0.62	40	4.18	2.54	1.6
A901	2.0	0.42	65	1.8	27	0.77	50	2.29	1.66	1.4
A92R	2.0	0.50	77	6.5	97	1.34	87	4.81	2.60	1.8

^a Wild-type and mutant yeast cells (20) were grown in a medium containing galactose and mitochondria isolated as described (21). The *bc*₁ complex was isolated from detergent-solubilized SMPs as described under Materials and Methods. Cytochrome *c* reductase activity and cytochrome content were determined spectrophotometrically as described (20). ^b Doubling time (hours).

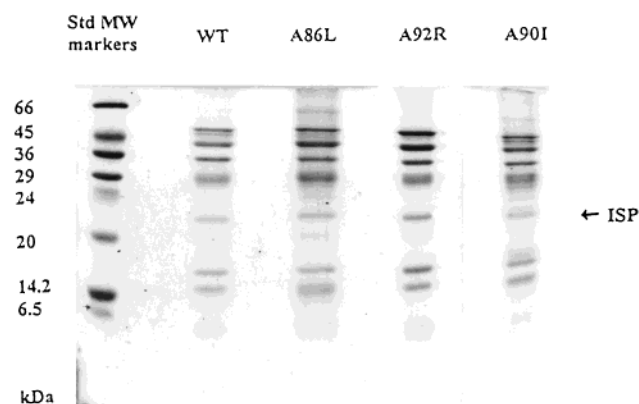


FIGURE 3: SDS–PAGE of the purified cytochrome *bc*₁ complexes isolated from wild-type and mutants in the tether region of the iron–sulfur protein. The purified proteins were separated by SDS–PAGE on 15% acrylamide gels and stained with Coomassie Blue. Lanes 1–5 (from left to right): 1, molecular weight marker proteins; 2, wild-type; 3, A86L; 4, A92R; 5, A901. The position of the iron–sulfur protein is indicated by an arrow.

(10–14, 17). Possibly, substitution of the bulky leucine residue for alanine might result in changes in the stigmatellin (ubiquinol) binding pocket leading to a loss of sensitivity to this inhibitor in the mutant. The inhibitory effects of stigmatellin on the cytochrome *c* reductase activity were determined in SMPs isolated from both the wild-type and the A86L mutant (Figure 5). A maximum inhibition of 65–70% was observed at a concentration of 8 nM stigmatellin for both wild-type and mutant A86L. Further increasing the stigmatellin concentration did not lead to further inhibitory effects. The lack of complete inhibition by stigmatellin was surprising as both antimycin and myxothiazol inhibited greater than 90% the cytochrome *c* reductase activity of the purified *bc*₁ complexes.

EPR spectroscopy has also been used to characterize the binding pocket for the 2Fe2S cluster on the iron–sulfur protein. The 2Fe2S cluster in the A86L mutant mitochondrial membranes reduced by ascorbate exhibited an EPR spectrum identical to that observed for the wild-type complex with resonances at $g_x = 1.8$ and at $g_y = 1.89$ (Figure 6). These results indicate that substituting leucine for alanine at position 86 did not change the microenvironment of the 2Fe2S cluster. Similarly, the EPR spectra of both the wild-type and the A86L mutant determined in the presence of stigmatellin were identical. The characteristic shift of the g_x value from 1.805 to 1.791 was observed in both complexes, suggesting that substitution of the bulky leucine for alanine at residue 86 of

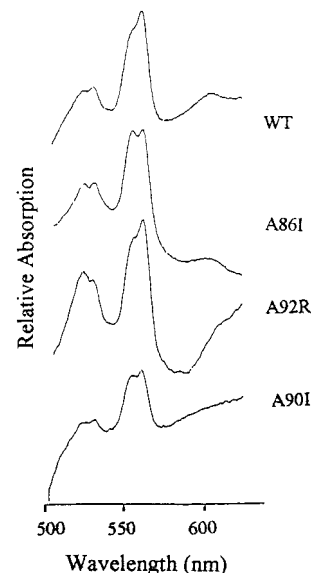


FIGURE 4: Spectral analysis of the cytochrome content of the cytochrome *bc*₁ complex isolated from wild-type and mutants in the tether region of the iron–sulfur protein. The *bc*₁ complexes were isolated from mitochondria obtained from wild-type and mutant yeast cells. Difference spectra of the dithionite-reduced minus ferricyanide-oxidized samples were recorded at room temperature.

the yeast iron–sulfur protein does not affect the Q_o pocket where ubiquinol is oxidized (23). These results are consistent with the observation that Ala-86 is located approximately 35 Å from the 2Fe2S cluster (10).

Proton Translocation Activity in Wild-Type and Mutant A86L. We wondered whether substituting leucine for alanine in the tether region of the iron–sulfur protein might have a differential effect on the rates of proton movement that accompany electron transfer in the *bc*₁ complex. Both the rate of electron transfer determined as cytochrome *c* reductase and the rate of proton movements measured as pH changes were compared in proteoliposomes containing the *bc*₁ complexes isolated from wild-type and mutant A86L (Table 2). The rate of electron transfer in the *bc*₁ complex isolated from mutant A86L was decreased 66% compared to the wild-type complex, a decrease similar to that observed with the isolated soluble *bc*₁ complex. The rate of proton pumping by the *bc*₁ complex isolated from both wild-type and mutant A86L mitochondria was double that of electron transfer, indicating a ‘classical’ H⁺/e[−] ratio of 2.0. The rate of proton pumping by the *bc*₁ complex isolated from mutant A86L, however, was decreased 55% compared to that of the wild-

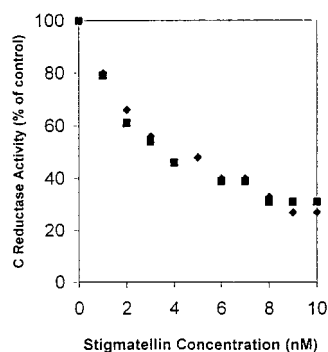


FIGURE 5: Inhibition of cytochrome *c* reductase activity of submitochondrial particles by stigmatellin. The SMPs (60 μ g) isolated from wild-type and mutant A86L were added to the reaction buffer containing 50 mM Tris·HCl, pH 7.4, 250 mM sucrose, and 1 mM EDTA and incubated with the indicated concentrations of stigmatellin for 5 min at 4 °C prior to addition of DBH₂ and determination of enzymatic activity. Wild-type (■) and mutant A86L (◆). Starting (100%) activity of the wild-type, 0.75 unit/mg; and for A86L, 0.33 unit/mg.

Table 2: Electron Transfer and Proton-Pumping Activities in the Cytochrome *bc*₁ Complex Isolated from Wild-Type and Mutant A86L Yeast Cells^a

strain	electron transfer rate	proton pumping	
		rate	+CCCP
wild-type	1.30 ± 0.27	2.60 ± 0.50	1.51 ± 0.45
A86	0.44 ± 0.28	1.18 ± 0.47	0.65 ± 0.41

^a Fifty microliters of purified *bc*₁ complex isolated from wild-type and mutant A86L mitochondria containing 0.5 nmol of cytochrome *b* was incorporated into proteoliposomes as described under Materials and Methods. Proton pumping was measured after addition of 150 μ M DBH₂ to the reaction mixture by the decrease in absorbance at 558 nm of 50 mM Phenol Red, while cytochrome *c* reductase activity was determined at 550 nm in the same mixture minus Phenol Red.

type. This loss of proton-pumping activity parallels the loss of electron transfer in the *bc*₁ complex isolated from this mutant (Table 1) and indicates that proton movements in mutant A86L are coupled to electron transfer. This conclusion is further supported by the observation that addition of the uncoupler CCCP to the incubation mixture decreased by nearly 50% the rate of proton pumping in both the wild-type and mutant complexes. It has been well established that uncouplers affect the release of electrogenic protons but not the release of the scalar protons from the quinol substrate during its oxidation by a Q-cycle mechanism (24).

Molecular Modeling of the Tether Region of the Iron–Sulfur Protein. The effects of mutating the conserved alanine residues, 86 and 92, in the iron–sulfur protein of yeast mitochondria were further investigated by computer modeling. Simulations of the *bc*₁ complexes isolated from wild-type and mutants A86L and A92R were performed using the same parameters, wherein hydrogens were added to all atoms, potentials were fixed, and the algorithm of steepest descent was selected utilizing the constant valence force field. Dynamics calculations were performed at 300 K for 5000 steps after 100 iterations of equilibration. All atoms of residues 83 through 93 of the yeast iron–sulfur protein (residues 63–73 in the bovine iron–sulfur protein) were allowed free range of motion, while all other atoms of the *bc*₁ complex were held fixed over the course of the simulations. Prior examination ensured that no fixed residues

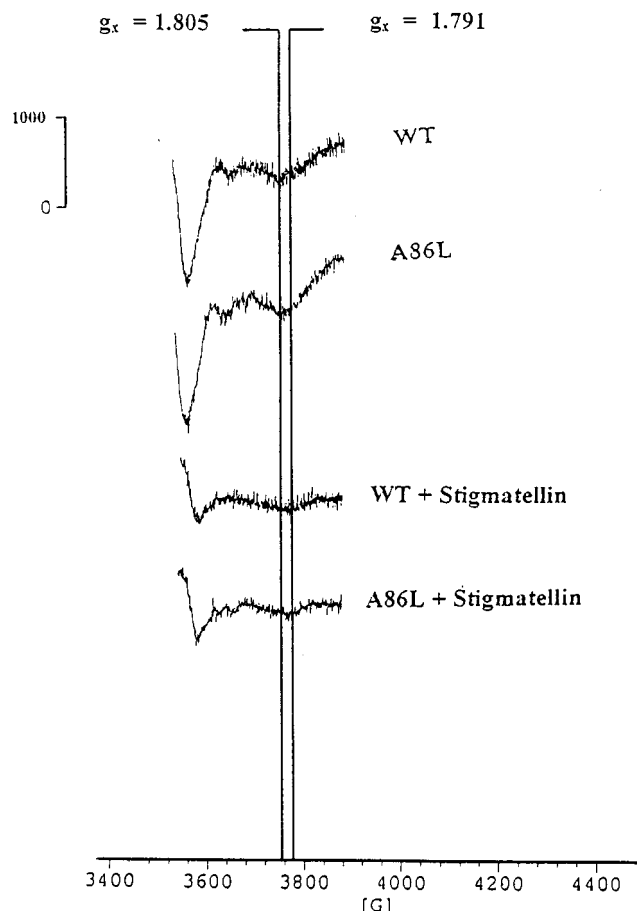


FIGURE 6: EPR spectra of the [2Fe-2S] cluster of the Rieske iron–sulfur protein in the wild-type and mutant A86L. SMPs (40 mg) isolated from wild-type and mutant A86L cells were resuspended in 0 mM potassium phosphate, pH 7.5, in 0.9% KCl buffer and reduced with 20 mM ascorbate at 0 °C for 10 min under anaerobic conditions and frozen in liquid nitrogen prior to EPR. Spectra were also recorded in the presence of 25 μ M stigmatellin as indicated on the traces. EPR conditions were as follows: temperature, 77 K; microwave power, 0.005 mW; modulation amplitude, 6.0 G; modulation frequency, 100 kHz; and microwave frequency, 9.398 GHz.

were within 12 Å of the mutated amino acids to ensure that any atom that might have an interaction with the mutation would be able to do so.

The computer simulations indicate that neither mutation A86L nor mutation A92R affects the α -helix backbone (blue ribbon) present in the tether region of the iron–sulfur protein (Figure 7). By contrast, closer examination of the model for the A86L mutant reveals that the side chain of leucine substituted at this position (highlighted in red) interacts with atoms of the leucine at residue 89 (in yellow) present in both the yeast and bovine iron–sulfur proteins. Two sets of hydrogen atoms located on these leucine residues are observed to be located within 2.6 Å of each other. These results suggest that this proximity may lead to decreased flexibility of the tether due and hence the 50% loss of activity observed in mutant A86L. Movement of the tether region requires unwinding of the small α -helix present in this region, which may be impeded as a result of the interactions of the two leucine side chains. It should be noted that substituting a cysteine residue for Ala-86 did not affect enzymatic activity of the *bc*₁ complex (20).

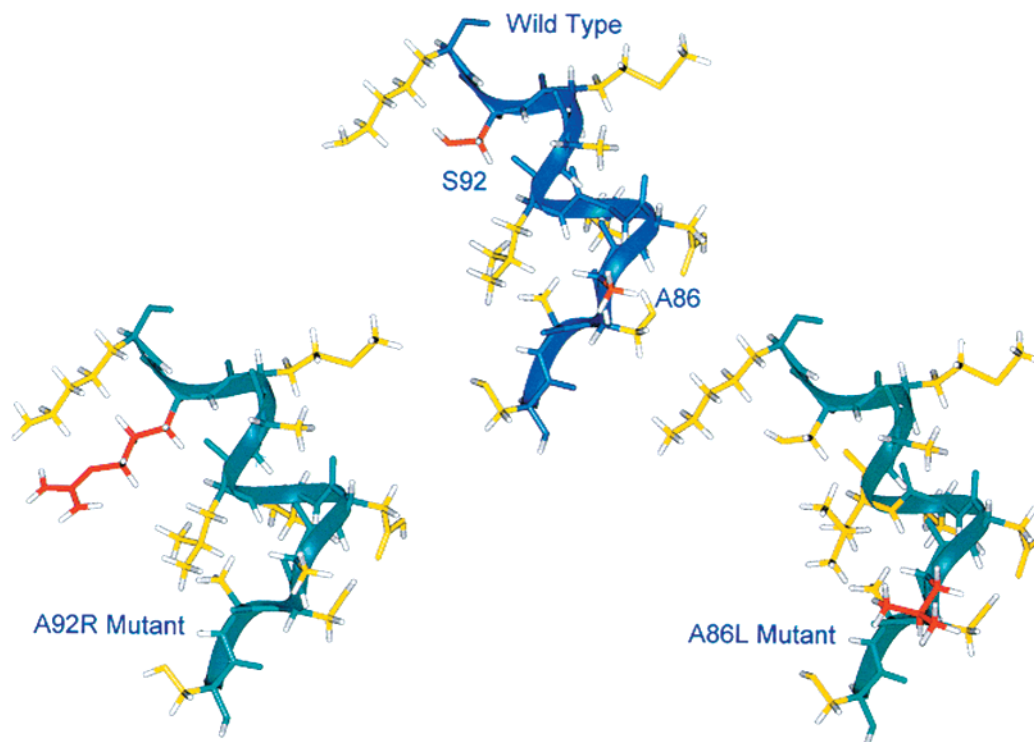


FIGURE 7: Molecular modeling of the tether region of the yeast iron–sulfur protein. Residues 83–93 (using the yeast numbering system) of the yeast iron–sulfur protein were subjected to computer simulations as described under Materials and Methods. The backbone of the α -helix is shown in dark blue for the wild-type and mutants A86L and A92R. The amino acid side chains are shown as yellow wire-frame models. In the wild-type, Ala-86 and Ser-92 (Ala-92 in yeast) are shown as red wire-frame stick models, while the amino acids substituted at residues 86 and 92 by site-directed mutagenesis are shown as red wire-frame models.

By contrast, the computer simulations indicate that the arginine substituted for Ala-92 (highlighted in red) did not interact with any other amino acids or change the conformation of the tether region of the iron–sulfur protein (Figure 7). It should be noted that a serine residue is present at position 92 in the bovine iron–sulfur protein indicated in orange in Figure 7. These results are consistent with the observation that substitution of an arginine for Ala-92 had no effect on the activity of the *bc*₁ complex.

Determination of Activation Energy for the *bc*₁ Complex from Wild-Type and Mutant A86L. To test the possibility that the loss of activity in mutant A86L results from steric hindrance due to the interaction of the substituted Leu-86 with Leu-89, the activation energy for ubiquinol to cytochrome *c* reductase was compared in the *bc*₁ complexes isolated from the wild-type and the mutants A86L and A92R. The Arrhenius plots for the purified *bc*₁ complex isolated from wild-type cells revealed a straight line (Figure 8) for which an activation energy of 55.38 kJ/mol was calculated, a value similar to that previously published for the yeast *bc*₁ complex (25). By contrast, the Arrhenius plot for the complex isolated from A86L was biphasic with an apparent transition observed at 17–19 °C. An activation energy of 279.8 kJ/mol was calculated for the slope obtained at temperatures below 17 °C, while an activation energy of 125.1 kJ/mol was calculated for the slope obtained at temperatures above 17 °C. Drawing a single slope for the entire temperature range from 10 to 25 °C resulted in a calculated activation energy of 204.7 kJ/mol (data not shown). The increased activation energy observed for the A86L mutant compared to the wild-type may result from decreased movement of the headgroup of the iron–sulfur protein due to the interac-

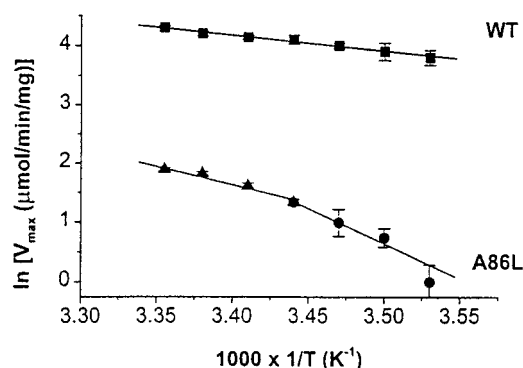


FIGURE 8: Arrhenius plots of the temperature dependence of cytochrome *c* reductase activity of the wild-type and mutant A86L. One slope is observed for the wild-type at temperatures ranging from 10 to 25 °C. Two slopes are observed for mutant A86L with an apparent transition at 17–18 °C. Correlation coefficients determined for the two slopes drawn above and below 17 °C for mutant A86L were -0.97975 and -0.97037 , respectively. Both of these values are more statistically significant than the correlation coefficient of -0.96815 determined for a single line drawn using the entire temperature range studied for mutant A86L.

tion of Leu-86 and Leu-89, which may directly result in an increased rigidity of the tether. The transition temperature observed at 17 °C is consistent with a large increase in molecular motion in proteins above this temperature.

By contrast, Arrhenius plots of the *bc*₁ complex isolated from mutant A92R revealed an activation energy of 79.89 kJ/mol, a value only slightly greater than that obtained for the *bc*₁ complex from wild-type mitochondria (data not shown). This result supports the computer simulation revealing that the arginine residue substituted for Ala-92 did not interact with any other residues of the tether region con-

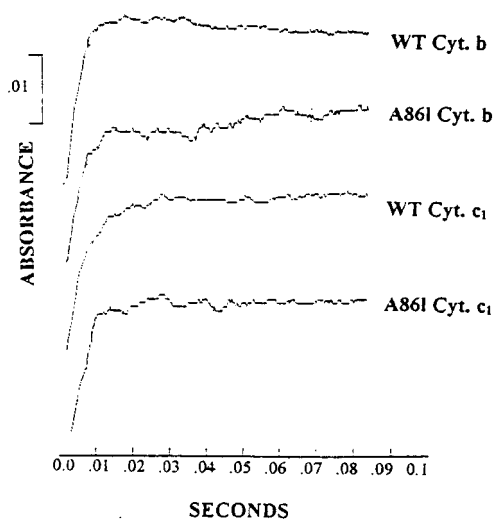


FIGURE 9: Initial rates of cytochrome *b* (563 nm) and *c*₁ (554 nm) reduction in wild-type and mutant A86L. The pre-steady-state rates were determined at room temperature by rapid-scanning stopped-flow spectroscopy as described under Materials and Methods. Reactions were started by mixing SMPs obtained from either the wild-type or mutant A86L in a buffer system containing 1 μ M antimycin with an equal volume of buffer containing 150 μ M DBH₂. A representative trace is shown in the figure. The initial rates were calculated by averaging 4–6 different reactions.

necting the headgroup with the membrane-spanning helix of the iron–sulfur protein. A similar increase in activation energy was reported in mutants of *R. sphaeroides* in which amino acid residues Pro-Leu-Pro were substituted for the sequence Ala-Leu-Ala in the tether region of the iron–sulfur protein (17). In chromatophores, the activation energy for cytochrome *c* reductase activity in this mutant was 69 kJ/mol as compared to the 24.7 kJ/mol observed for the wild-type chromatophores.

Initial Kinetics of Cytochrome *b* and *c*₁ Reduction in Mitochondria from Wild-Type and Mutant A86L Strains. The computer simulations and activation energy calculations have suggested that the decrease in enzymatic activity observed in the *bc*₁ complex in mutant A86L may result from a steric hindrance and thus decreased movement of the tether region of the iron–sulfur protein. This suggestion prompted us to investigate the initial rates of cytochrome *b* and *c*₁ reduction in the mutant compared to the wild-type under single-turnover conditions to learn whether the A86L mutation affects differentially the reduction of cytochrome *b* or cytochrome *c*₁. The pre-steady-state kinetic experiments were performed with DBH₂ as substrate in the presence of antimycin to block further oxidation/reduction of cytochrome *b* at center N. Under these conditions, the reduction of both cytochromes *b* and *c*₁ was biphasic in SMPs isolated from wild-type and mutant A86L (Figure 9). The initial rate of the rapid phase of cytochrome *b* reduction was 125 ± 2.2 s^{−1} in the wild-type. A similar rate of cytochrome *b* reduction of 130 ± 19.4 s^{−1} was observed in the SMPs from mutant A86L. By contrast, the initial rate of the rapid phase of cytochrome *c*₁ reduction in the A86L mutant was 73 ± 2.8 s^{−1}, a decrease of 33% compared to the rapid phase of *c*₁ reduction in the wild-type of 109 ± 17.1 s^{−1}. The decrease in the pre-steady-state reduction rates for the fast phase of cytochrome *c*₁ reduction, while significant, was not as great as the 60% inhibition observed in the steady-state reduction

of cytochrome *c* observed in both mitochondria and the purified *bc*₁ complex of mutant A86L. It should be pointed out that this decrease is indeed significant when compared to the observation that the initial rate of cytochrome *b* reduction in the A86L mutant was unchanged compared to the wild-type. Steric hindrance due to the leucine substituted for alanine would be expected to impede the unwinding of the α -helix with a resultant loss of flexibility and hence movement of the tether toward cytochrome *c*₁. Decreased motion in the tether of the mutant iron–sulfur proteins would be reflected in lowered rates of electron transfer from the iron–sulfur protein to cytochrome *c*₁. Decreased motion in the tether region of the iron–sulfur protein, however, would not be expected to affect the rate of electron transfer from the iron–sulfur protein in the ‘*b*’ state to cytochrome *b* in the Q₀ site. These experiments are initiated with the iron–sulfur protein in the oxidized state and the reaction started by addition of reduced quinol, which would facilitate the docking of the iron–sulfur protein to cytochrome *b*. Similar differences in the rates of cytochromes *b* and *c*₁ were recently obtained with the *bc*₁ complex of *R. capsulatus* in which addition of 1–2 alanine residues in the tether region of the iron–sulfur protein resulted in decreases in the rate of cytochrome *c*₁ reduction but not of cytochrome *b* reduction (21). Moreover, the decreased rate of cytochrome *c*₁ reduction was correlated with loss of the postulated movement of the tether region of the iron–sulfur protein. Apparently, under these experimental conditions, movement of the tether is more critical for rapid rates of cytochrome *c*₁ reduction than for cytochrome *b* reduction.

CONCLUSION

Substituting a leucine residue for the conserved Ala-86 located in the tether region of the yeast iron–sulfur protein resulted in a 50% or greater loss of cytochrome *c* reductase activity without loss of protein or heme and without changes in the 2Fe2S cluster in either mitochondrial membranes or the isolated *bc*₁ complex. Moreover, this mutation did not impede the ability of the isolated *bc*₁ complex to translocate protons across the membrane and establish a membrane potential. Computer simulations have indicated that the side chain of the leucine substituted for Ala-86 may interact with the side chain of Leu-89. We suggest that the close proximity of several hydrogen atoms present in the side chains of the two leucine residues may impede the unwinding of the α -helix located in the tether region necessary for movement of the headgroup of the iron–sulfur protein. Consequently, mutant A86L had lowered activity of the *bc*₁ complex. This suggestion is supported by the higher activation energies calculated for the mutant A86L compared to the wild-type at all temperatures. Moreover, the apparent biphasic nature of the Arrhenius plot observed for mutant A86L provides further evidence for the suggestion that steric hindrance causes the loss of enzymatic activity in mutant A86L of the iron–sulfur protein.

ACKNOWLEDGMENT

We thank Dr. Michael Gunther of the Department of Biochemistry for his help in the EPR experiments and Dr. Grazyna Szklarz of the Department of Pharmaceutical Sciences in the School of Pharmacy at West Virginia

University for her help in the molecular modeling studies. All molecular simulations were performed in the West Virginia University Computational Chemistry and Molecular Modeling Laboratory in the Department of Basic Pharmaceutical Sciences.

REFERENCES

1. Trumpower, B. L., and Gennis, R. B. (1994) *Annu. Rev. Biochem.* 63, 675–716.
2. Brandt, U., and Trumpower, B. L. (1994) *Crit. Rev. Biochem. Mol. Biol.* 29, 165–197.
3. DiRago, J. P. O., Bruel, C., Graham, P., Slonimski, B. L., and Trumpower, B. L. (1996) *J. Biol. Chem.* 271, 15341–15345.
4. Yu, C.-A., Xia, D., Kim, H., Deisenhofer, J., Zhang, L., Kachurin, A. M., and Yu, L. (1998) *Biochim. Biophys. Acta* 1365, 151–158.
5. Mitchell, P. (1976) *J. Theor. Biol.* 62, 327–367.
6. Trumpower, B. L. (1990) *J. Biol. Chem.* 265, 11409–11412.
7. Crofts, A. R., and Meinhardt, S. W. (1982) *Biochem. Soc. Trans.* 10, 201–203.
8. Xia, D., Yu, C. A., Kim, H., Xia, J. Z., Kachurin, A. M., Zhang, L., Yu, L., and Deisenhofer, J. (1997) *Science* 277, 60–66.
9. Iwata, S., Lee, J. W., Okada, K., Lee, J. K., Iwata, M., Rasmussen, B., Link, T. A., Ramaswamy, S., and Jap, B. K. (1998) *Science* 281, 64–71.
10. Zhang, Z., Huang, L., Shulmeister, V. M., Chi, Y. I., Kim, K. K., Hung, L. W., Crofts, A. R., Berry, E. A., and Kim, S. H. (1998) *Nature* 392, 677–684.
11. Hunte, C., Koepke, J., Lange, C., Rossmanith, T., and Michel, H. (2000) *Struct. Fold. Des.* 8, 669–684.
12. Crofts, A. R., and Berry, E. A. (1998) *Curr. Opin. Struct. Biol.* 8, 677–684.
13. Crofts, A. R., Guergova-Kuras, M., Huang, L. S., Kuras, R., Zhang, Z., and Berry, E. A. (1999) *Biochemistry* 38, 15791–15806.
14. Crofts, A., Barquera, B., Gennis, R. B., Kuras, R., Guergova-Kuras, M., and Berry, E. A. (1999) *Biochemistry* 38, 15807–15826.
15. Snyder, C. H., Gutierrez-Cirlos, E. B., and Trumpower, B. L. (2000) *J. Biol. Chem.* 275, 13535–13541.
16. Graham, L. A., and Trumpower, B. L. (1991) *J. Biol. Chem.* 266, 22485–22492.
17. Tian, H., Yu, L., Mather, M. W., and Yu, C. A., (1998) *J. Biol. Chem.* 273, 27953–27959.
18. Tian, H., White, L., Yu, L., and Yu, C. A. (1999) *J. Biol. Chem.* 274, 7146–7152.
19. Darrouzet, E., Valkova-Valchanova, M., Ohnishi, T., and Daldal, F. (1999) *J. Bioenerg. Biomembr.* 31, 275–288.
20. Obungu, V. H., Wang, Y., Amyot, S. M., Gocke, C. B., and Beattie, D. S. (2000) *Biochim. Biophys. Acta* 1457, 36–44.
21. Darrouzet, E., Valkova-Valchanova, M., Moser, C. C., Dutton, P. L., and Daldal, F. (2000) *Proc. Natl. Acad. Sci. U.S.A.* 97, 4567–4572.
22. Fu, W., and Beattie, D. S. (1991) *J. Biol. Chem.* 266, 14958–14963.
23. Ding, H., Robertson, D. E., Daldal, F., and Dutton, P. L. (1992) *Biochemistry* 31, 3144–3158.
24. Beattie, D. S., and Villalobo, A. (1982) *J. Biol. Chem.* 257, 14745–14752.
25. Brandt, U., and Okun, J. G. (1997) *Biochemistry* 36, 11234–11240.

BI001708T